Article

General Method for Ultrathin Free-Standing Films of Nanofibrous Composite Materials

Xinsheng Peng, Jian Jin, Emma M. Ericsson, and Izumi Ichinose

J. Am. Chem. Soc., **2007**, 129 (27), 8625-8633• DOI: 10.1021/ja0718974 • Publication Date (Web): 15 June 2007

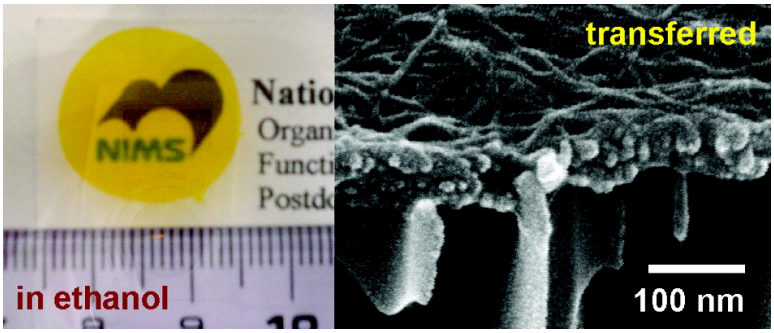

More About This Article

Additional resources and features associated with this article are available within the HTML version:

- Supporting Information
- Links to the 4 articles that cite this article, as of the time of this article download
- Access to high resolution figures
- Links to articles and content related to this article
- Copyright permission to reproduce figures and/or text from this article

View the Full Text HTML

J|A|C|S
ARTICLES
Published on Web 06/15/2007

General Method for Ultrathin Free-Standing Films of Nanofibrous Composite Materials

Xinsheng Peng,[†,‡] Jian Jin,[†] Emma M. Ericsson,[†] and Izumi Ichinose*[,†]

Contribution from the Organic Nanomaterials Center and International Center for Young Scientists, National Institute for Materials Science (NIMS), 1-1 Namiki, Tsukuba, Ibaraki 305-0044, Japan

Received March 18, 2007; E-mail: ichnose.izumi@nims.go.jp

Abstract: A simple and general method for the preparation of ultrathin, large-area, free-standing films of nanofibrous composite materials was developed. First, positively charged cadmium hydroxide nanostrands of 1.9 nm in diameter and micrometers in length were prepared by mixing dilute aqueous solutions of cadmium chloride and aminoethanol. Negatively charged dye molecules, proteins, nanoparticles, and water-soluble fullerene or carbon nanotubes were mixed with the nanostrands to give a well-dispersed solution of the corresponding nanofibrous composites. After filtration of the dispersions with a polycarbonate membrane filter, uniform films with a thickness of a few tens to hundreds of nanometers and a diameter of a few centimeters were obtained. The films were readily peeled off from the membrane filter by immersion in ethanol. The resultant free-standing films could be further transferred to other substrates, such as quartz plate, gold electrode, and porous alumina membrane, and were characterized by scanning and transmission electron microscopies. We provide herein various nanofibrous free-standing films with optical, biological, metallic, and magnetic properties.

Introduction

The free-standing films with well-defined nanostructures have great potential for a broad range of applications such as separation membranes, sensors, and catalysts. They are versatile for use in electronic insulating, optical filtration, photoenergy conversion, adsorption of viruses, and biomaterials.[1] The demand for the separation of reactive gases such as methane and carbon monoxide is rapidly increasing with the present energy and environmental issues. The permeation of molecules through microporous thin films often shows interesting phenomena, in which physics and chemistry are complicatedly involved.[2]

There are many ways to prepare free-standing films with desirable structures, which can be categorized in the following four types. The first type is conventional methods, including solution casting,[3] plasma sputtering,[4] chemical or physical vapor deposition,[5] and spin-coating on a planar solid surface.[6] Very thin films are usually prepared on a sacrificial layer such as silicon oxide and organic polymers, which are readily removed by treating with hydrofluoric acid or organic solvents. For example, Whitesides et al. have reported geometrically well-defined free-standing films prepared by using a poly(dimethylsiloxane) (PDMS) stamp and by subsequent chemisorption of polymers and etching of the substrate.[7] Kunitake et al. prepared nanometer-thick, large-area, free-standing films of organic−inorganic hybrids through spin-coating on a sacrificial layer of polyvinylphenol.[8] Erik and his co-workers polymerized self-assembled monolayers (SAMs) on silicon nitride substrates. After treating them with hydrofluoric acid, monomolecular thick free-standing films were obtained.[9] The second type is methods using liquid interfaces. The Langmuir−Blodgett technique was often used for the preparation of free-standing films of polymeric surfactants.[10] Ozin and his co-workers have reported free-standing thin films of oriented mesoporous silica prepared at the air−water interface.[11] The preparation technique of black lipid membranes has been applied for the free-standing polymer films by Nardin et al.[12] We reported that the air-stable free-

[†] Organic Nanomaterials Center.
[‡] International Center for Young Scientists.

(1) (a) Baker, R. W. *Membrane Separation Systems*—Recent Developments and Future Directions; William Andrew Publishing: Noyes, NJ, 1991. (b) Henis, J. M. S.; Tripodi, M. K. *Science* **1983**, *220*, 11. (c) Jirage, K. B.; Hulteen, J. C.; Martin, C. R. *Science* **1997**, *278*, 655. (d) Decher, G.; Schlenoff, J. B. *Multilayer Thin Films: Sequential Assembly of Nanocomposite Materials*; Wiley-VCH: Weinheim, Germany, 2003. (e) Striemer, C. C.; Gaborski, T. R.; McGrath, J. L.; Fauchet, P. M. *Nature* **2007**, *445*, 749.
(2) (a) Holt, J. K.; Park, H. G.; Wang, Y.; Stadermann, M.; Artyukhin, A. B.; Grigoropoulos, C. P.; Noy, A.; Bakajin, O. *Science* **2006**, *312*, 1034. (b) Mulder, M. *Basic Principles of Membrane Technology*; Kluwer Academic Publishers: Dordrecht, Netherlands, 1991. (c) Lakshmi, B. B.; Martin, C. R. *Nature* **1997**, *388*, 758.
(3) (a) Mattsson, J.; Forrest, J. A.; Börjesson, L. *Phys. Rev. E* **2000**, *62*, 5187. (b) Dong, W.; Cogbill, A.; Zhang, T.; Ghosh, S.; Tian, Z. R. *J. Phys. Chem. B* **2006**, *110*, 16819.
(4) Peng, X.; Luo, Y.-H.; Jin, J.; Huang, J.; Ichinose, I.; Kurashima, K.; Papadimitrakopoulos, F. *Chem. Commun.* **2006**, 4688.
(5) Roberts, M. M.; Klein, L. J.; Savage, D. E.; Slinker, K. A.; Friesen, M.; Celler, G.; Eriksson, M. A.; Lagally, M. G. *Nat. Mater.* **2006**, *5*, 388.
(6) Jiang, C.; Markutsya, S.; Tsukruk, V. V. *Adv. Mater.* **2004**, *16*, 157.
(7) Huck, W. T. S.; Stroock, A. D.; Whitesides, G. M. *Angew. Chem., Int. Ed.* **2000**, *39*, 1058.
(8) Vendamme, R.; Onoue, S.; Nakao, A.; Kunitake, T. *Nat. Mater.* **2006**, *5*, 494.
(9) Eck, W.; Küller, A.; Grunze, M.; Völkel, B.; Gölzhäuser, A. *Adv. Mater.* **2005**, *17*, 2583.
(10) (a) Goedel, W. A.; Peyratout, C.; Ouali, L.; Schädler, V. *Adv. Mater.* **1999**, *11*, 213. (b) Mallwitz, F.; Goedel, W. A. *Angew. Chem., Int. Ed.* **2001**, *40*, 2645. (c) Endo, H.; Kado, Y.; Mitsuishi, M.; Miyashita, M. *Macromolecules* **2006**, *39*, 5559. (d) Xu, H.; Goedel, W. A. *Langmuir* **2002**, *18*, 2363. (e) McNamee, C. E.; Jaumann, M.; Möller, M.; Ding, A.; Hemeltjen, S.; Ebert, S.; Baumann, W.; Goedel, W. A. *Langmuir* **2005**, *21*, 10475.
(11) Yang, H.; Coombs, N.; Sokolov, I.; Ozin, G. A. *Nature* **1996**, *381*, 589.

standing films were obtainable after drying wet foam films of some amphiphilic compounds.[13] The third type is methods by means of layer-by-layer (LBL) adsorption of polyelectrolytes. The technique pioneered by G. Decher is nowadays widely employed for various free-standing films.[14] Kotov et al., for example, prepared mechanically strong free-standing films of clay/polyelectrolyte or carbon nanotube/polyelectrolyte mulilayers.[15] Tsukruk and his co-workers reported multilayer assemblies of polyelectrolytes and metal nanoparticles and their sensing properties.[16]

The fourth type is based on the filtration of nanofibrous materials. This is close to the method for paper manufacturing by using microfibers of cellulose.[17] Wu and his co-workers fabricated transparent, conductive, free-standing films of single-walled carbon nanotubes (SWCNT) by filtering the dispersed solution on a mixed cellulose ester membrane filter.[18] Zhou et al. also prepared free-standing SWCNT films by filtration. They demonstrated that the films could be readily transferred from a membrane filter to other substrates by using a PDMS stamp.[19] The filtration method provides a simple and easy way to prepare large-scale free-standing films. The thickness is controlled by the volume of the filtered dispersion. Furthermore, it is not necessary to design chemical interaction between substrate and nanofibrous materials. However, this method requires materials of very high aspect ratio, and they also need to be dispersible in the solvent and rigid enough to be stable for suction filtration. Because of these requirements, it has been hard to find proper nanofibrous materials except for carbon nanotubes.

We reported that cadmium hydroxide nanostrands were formed just by raising the pH of the aqueous solution of cadmium nitrate.[20] This nanostrand had a diameter of 1.9 nm, and the length reached a few micrometers. A similar nanostrand was recently found for copper hydroxide.[21] The nanostrands are highly dispersible in water, since the surfaces are extremely positively charged. For example, about one-sixth of the cadmium atoms in the nanostrand are presumed to be positively charged. This value corresponds to one-third of the surface cadmium atoms. Such a feature has been applied for capturing short DNA fragments and designing supramolecular assemblies with negatively charged dye molecules.[22] Metal hydroxide nanostrands satisfy all the requirements for the above filtration method. We have briefly reported that cadmium hydroxide nanostrands were able to be filtered off by using a porous substrate, just the same as carbon nanotubes.[4] However, the nanostrands were not mechanically very stable so that it was hard to obtain their free-standing films larger than a hundred micrometers.

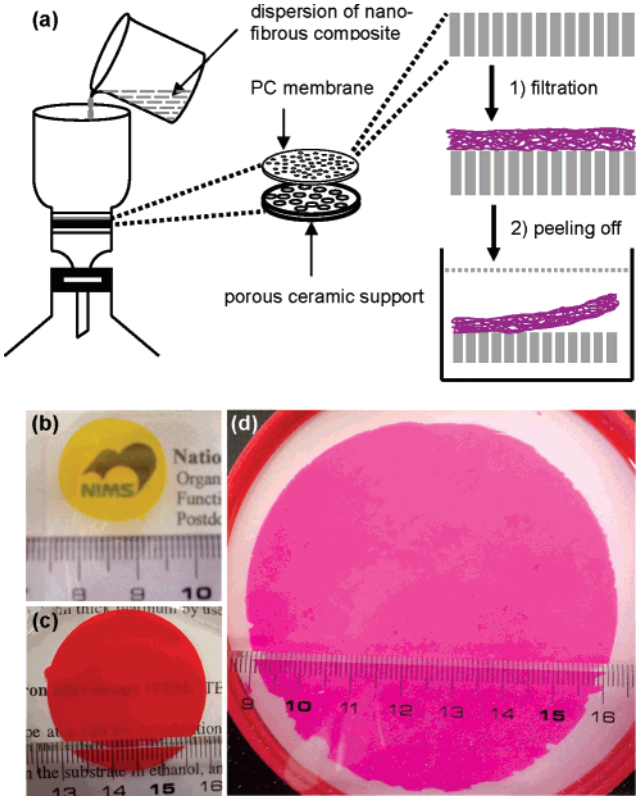

Figure 1. Preparation of ultrathin nanofibrous free-standing films (a) and their photographs (b−d). The film size is 1.9 cm (b), 3.2 cm (c), and 7.5 cm (d), respectively. These films (b−d) were prepared from the dispersions of cadmium hydroxide nanostrands containing direct yellow 50 (DY), congo red (CR), or sulforhodamine G (SRG). The preparation conditions correspond to DY-2, CR-4, and SRG-1 in Table 1.

In this article, we prepared a wide range of nanocomposites of cadmium hydroxide nanostrands and examined them as structural components of free-standing films. Interestingly, the mechanical property of the films was significantly improved by forming the nanocomposites. As a result, we could successfully develop a simple and general method for the preparation of nanofibrous free-standing films. In spite of the thickness of a few tens of nanometers, the size was beyond a few centimeters. Moreover, the generality of this method made it possible to provide various functional free-standing films.

Results and Discussion

Preparation of Free-Standing Films by Filtration. Cadmium hydroxide nanostrands were synthesized by mixing equal volume of aqueous solutions of 4 mM $CdCl_2$ and 0.8 mM 2-aminoethanol under vigorous stirring.[20] After allowing to stand for 10 min, an aqueous solution of negatively charged compound (dye molecule, protein, nanoparticle, and water-soluble fullerene or carbon nanotube) was added, and the mixture was stirred for 30 min. The solution tuned to a weakly gelled dispersion, probably due to the networking of the nanostrands and negatively charged compound. Then, a certain volume of the dispersion was filtered on a polycarbonate (PC) membrane filter with pores of 0.2 μm. As shown in Figure 1a, the membrane filter locates on a porous ceramic support of a filtration funnel. Suction filtration was performed at decreasing pressure from

(12) Nardin, C.; Winterhalter, M.; Meier, W. *Langmuir* **2000**, *16*, 7708.
(13) Jin, J.; Huang, J.; Ichinose, I. *Angew. Chem., Int. Ed.* **2005**, *44*, 4532.
(14) (a) Decher, G. *Science* **1997**, *277*, 1232. (b) Dubas, S. T.; Farhat, T. R.; Schlenoff, J. B. *J. Am. Chem. Soc.* **2001**, *123*, 5368. (c) Ono, S. S.; Decher, G. *Nano Lett.* **2006**, *6*, 592. (d) Mallwitz, F.; Laschewsky, A. *Adv. Mater.* **2005**, *17*, 1296. (e) Nolte, M.; Schoeler, B.; Peyratout, C. S.; Kurth, D. G.; Fery, A. *Adv. Mater.* **2005**, *17*, 1665.
(15) (a) Tang, Z.; Kotov, N. A.; Magonov, S.; Ozturk, B. *Nat. Mater.* **2003**, *2*, 413. (b) Mamedov, A. A.; Kotov, N. A.; Prato, M.; Guidi, D. M.; Wicksted, J. P.; Hirsch, A. *Nat. Mater.* **2002**, *1*, 190.
(16) (a) Jiang, C.; Tsukruk, V. V. *Adv. Mater.* **2006**, *18*, 829. (b) Jiang, C.; Markutsya, S.; Pikus, Y.; Tsukruk, V. V. *Nat. Mater.* **2004**, *3*, 721.
(17) (a) Zheng, Z.; McDonald, J.; Khillan, R.; Su, Y.; Shutava, T.; Grozdits, G.; Lvov, Y. M. *J. Nanosci. Nanotechnol.* **2006**, *6*, 1. (b) Lvov, Y. M.; Grozdits, G. A.; Eadula, S.; Zheng, Z.; Lu, Z. *Nord. Pulp Pap. Res. J.* **2006**, *21*, 552.
(18) Wu, Z.; Chen, Z.; Du, X.; Logan, J. M.; Sippel, J.; Nikolou, M.; Kamaras, K.; Reynolds, J. R.; Tanner, D. B.; Hebard, A. F.; Rinzler, A. G. *Science* **2004**, *305*, 1273.
(19) Zhang, D.; Ryu, K.; Liu, X.; Polikarpov, E.; Ly, J.; Tompson, M. E.; Zhou, C. *Nano Lett.* **2006**, *6*, 1880.
(20) Ichinose, I.; Kurashima, K.; Kunitake, T. *J. Am. Chem. Soc.* **2004**, *126*, 7162.
(21) Luo, Y.-H.; Huang, J.; Jin, J.; Peng, X.; Schmitt, W.; Ichinose, I. *Chem. Mater.* **2006**, *18*, 1795.
(22) (a) Ichinose, I.; Huang, J.; Luo. Y.-H.; *Nano Lett.* **2005**, *5*, 97. (b) Luo, Y.-H.; Huang, J.; Ichinose, I. *J. Am. Chem. Soc.* **2005**, *127*, 8296.

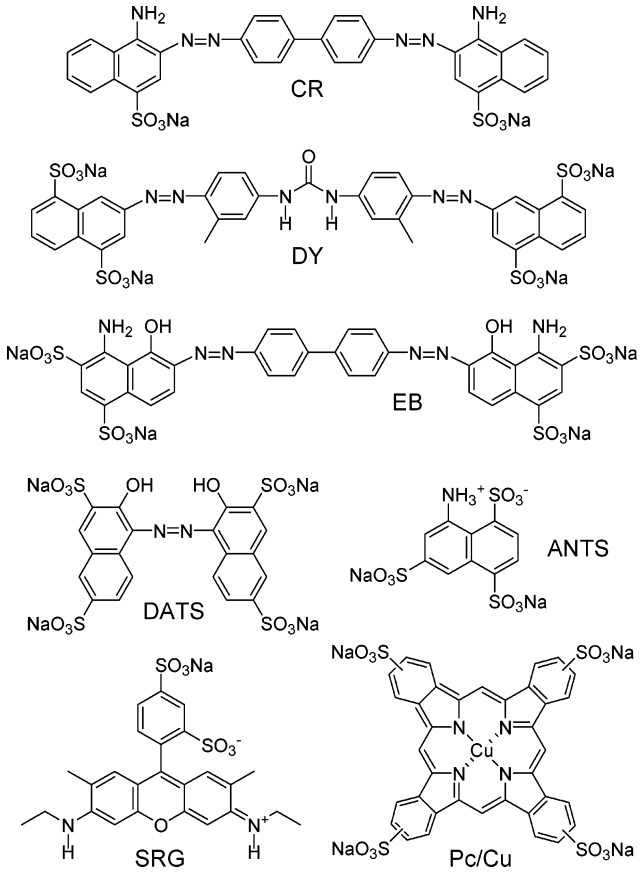

Figure 2. Structures of congo red (CR), direct yellow 50 (DY), Evans blue (EB), 2,2′-dihydroxy-1,1′-azonaphthalene-3,3′,6,6′-tetrasulfonic acid tetrasodium salt (DATS), 8-aminonaphthalene-1,3,6-trisulfonic acid disodium salt (ANTS), sulforhodamine G (SRG), and copper phthalocyanine tetrasulfonic acid tetrasodium salt (Pc/Cu).

atmosphere to 10 kPa. The filtration usually completed within 3 min. Subsequently, the film was peeled off from the membrane filter by immersion in ethanol.

The thickness of the free-standing films depends on the volume of the filtered solution and the size of the filtration funnel. In our system, 10 mL of the dispersion gave a thickness of about 40 nm by using a 1.9 cm funnel. The photographs of free-standing films prepared by 1.9, 3.2, and 7.5 cm funnels are shown in Figure 1. The size is equal to the diameter of the filtration funnels, which indicates that the films do not shrink before and after peeling off. Unless otherwise stated, the free-standing films in this article were prepared by using a 1.9 cm funnel. For further characterization, the films were often transferred to other substrates, such as quartz plate, gold electrode, porous alumina membrane, etc., by immersing the substrate under a floating free-standing film and by carefully lifting.

Free-Standing Films of Dye/Nanostrand Composites. We first examined the versatility of this technique for various dye molecules. The structures are shown in Figure 2. Congo red (CR), direct yellow 50 (DY), and Evans blue (EB) contain two azobenzene units and two or four sulfonate groups. 2,2′-Dihydroxy-1,1′-azonaphthalene-3,3′,6,6′-tetrasulfonic acid tetrasodium salt (DATS) has one azobenzene unit. Besides azobenzene dyes, 8-aminonaphthalene-1,3,6-trisulfonic acid disodium salt (ANTS), sulforhodamine G (SRG), and copper phthalocyanine tetrasulfonic acid tetrasodium salt (Pc/Cu) were examined. These molecules have more than one negative charge at neutral pH conditions, except for SRG.

As mentioned above, cadmium hydroxide nanostrands were prepared at the molar ratio of 1/5 for aminoethanol against $CdCl_2$. Under this condition, about 10% of cadmium chloride is converted to the nanostrands. The low conversion ratio is important for the stabilization of cadmium hydroxide nanostrands and their composites with dye molecules, since the nanostrands are prone to precipitate with the increasing conversion ratio. As reported before, positively charged cadmium atoms are about one-sixth of the total cadmium atoms in the nanostrand.[22] Therefore, the amount of the positive charges can be estimated from the concentration of $CdCl_2$ and the above conversion ratio. In our experimental condition, the concentration was calculated to be 3.3×10^{-5} M. On the other hand, the concentration of dye molecules was set to be enough to electrostatically compensate the positive charges of the nanostrands. For example, 0.4 mL of 1 mM CR (congo red) was mixed with 20 mL of the nanostrand solution. CR has two sulfonate groups, so that the concentration of the sulfonate groups is about 3.9×10^{-5} M. After stirring 30 min, the mixed solution was suction filtered by using a PC membrane filter on a filtration funnel of 1.9 cm. These experimental conditions are listed in Table 1.

The CR/nanostrand composite was examined by scanning electron microscopy (SEM). As shown at the left of Figure 3a, the composite on a PC membrane filter had nanofibrous morphology. This image was obtained after coating 2 nm thick platinum layer to prevent electric charging. When the thickness was subtracted, the average width of nanofibers was estimated to be 13 nm. We also examined the assembly of the nanostrands in the mixed solution by transmission electron microscopy (TEM). A carbon-coated TEM microgrid was floated on the dispersion of CR/nanostrand composite, had the solution wiped from the edge of the grid, dried in vacuum, and subjected to TEM observation at the acceleration voltage of 100 kV. As shown at the right of Figure 3a, parallel arrangements of cadmium hydroxide nanostrands were observed all over the grid. The bundle-like assemblies are composed of 2−4 nanostrands. It is known that pure cadmium hydroxide nanostrands are isolated from each other in the aqueous solution.[20]

Therefore, the parallel arrangements must be induced by negatively charged CR molecules. The nanocomposite film was readily peeled off from the PC membrane filter by immersion in ethanol for 2 min. The photograph is shown in the inset of Figure 3a. The thickness of this transparent film was only 80 nm, as confirmed by cross-sectional SEM measurements (see below). The strong red color indicates that a great number of CR molecules are incorporated into the nanocomposite film. In fact, almost all the CR molecules were captured by the nanostrands, judging from the colorless filtrate.

Similar free-standing films were obtained by using DATS. In this case, we reduced the concentration to be half of that of CR, since the number of sulfonate groups were double that of CR. As shown in Figure 3b, the DATS/nanostrand composite gave a nanofibrous morphology. The width of the nanofiber was 11 nm, which was a little narrower than that of the CR/nanostrand composite probably due to the short molecular length. The transparent and slightly pink film had a thickness of 75 nm. DY (direct yellow 50) gave nanofibers with a width

Table 1. Preparation of Ultrathin Free-Standing Films Containing Dyes, Proteins, and Nanoparticles

Dye Solution

sample	dye	concn (mM)	volume (mL)	nanostrand solution (mL)	nanofiber width[a] (nm)	funnel diameter (cm)	thickness (nm)	corresponding images
CR-1	CR	1	0.2	10	13	1.9	40	Figure S1
CR-2	CR	1	0.3	15	13	1.9	60	Figure S1
CR-3	CR	1	0.4	20	13	1.9	80	Figure 3a
CR-4	CR	1	1.2	60	13	3.2	85	Figure 1c
DY-1	DY	1	0.1	10	14	1.9	40	Figure S1
DY-2	DY	1	0.15	15	14	1.9	60	Figure 1b, 3c, S1
EB-1	EB	1	0.05	5	15	1.9	20	Figure 3d, 4a−c
EB-2	EB	1	0.1	10	15	1.9	40	Figure 4c,d
EB-3	EB	1	0.2	20	15	1.9	82	Figure 4c
EB-4	EB	1	0.3	30	15	1.9	125	Figure 4c
EB-5	EB	1	0.6	60	15	1.9	245	Figure 4c
DATS	DATS	1	0.2	20	11	1.9	75	Figure 3b
SRG-1	SRG	1	12.8	320	17	7.5	80	Figure 1d
SRG-2	SRG	1	1.2	30	17	1.9	125	Figure 5a
Pc/Cu	Pc/Cu	1	0.3	30	10	1.9	120	Figure 5b
ANTS	ANTS	1	0.15	10	32	1.9	42	Figure 5c

Protein Solution[b]

sample	protein	concn (mg/ mL)	volume (mL)	nanostrand solution (mL)	nanofiber width[a] (nm)	funnel diameter (cm)	thickness (nm)	corresponding images
ferritin	ferritin	1	1	10	*c*	1.9	55	Figure 6a
Cyt.c	Cyt.c	1	1	10	8	1.9	45	Figure 6b
GOx	GOx	1	1	10	10	1.9	48	Figure 6c,d

Colloidal Particle Dispersion[d]

sample	material	diameter (nm)	volume (mL)	nanostrand solution (mL)	nanofiber width[a] (nm)	funnel diameter (cm)	thickness (nm)	corresponding images
Au-1	Au	2	6	30	8	1.9	115	Figure S2a
Au-2	Au	2	12	30	10	1.9	130	Figure 7a
Au-3	Au	10	3	30	*c*	1.9	125	Figure S2b
Au-4	Au	20	3	30	*c*	1.9	132	Figure S2c
Au-5	Au	20	9	30	*c*	1.9	140	Figure 7b
Au-6	Au	40	3	30	*c*	1.9	128	Figure S2d
Au-7	Au	40	12	30	*c*	1.9	150	Figure 7c
Fe_3O_4	Fe_3O_4	5	0.1	10	*c*	1.9	45	Figure 7d

[a] Average width of bundlelike nanocomposite fibers observed by SEM measurements. This width was obtained after subtracting the thickness of 2 nm platinum coating. [b] Protein solutions were adjusted to be pH 7.0 for ferritin, pH 11.0 for Cyt.c, and pH 7.0 for GOx by using hydrogen chloride and sodium hydroxide. Isoelectric points of these proteins are pI 4.5−4.8 (ferritin), pI 10.6 (Cyt.c), and pI 4.2 (GOx). [c] Because of the large particle sizes, the width of nanofibers was hard to determine. [d] Concentrations of these colloidal particles are 1.5×10^{14}, 5.7×10^{12}, 7×10^{11}, and 9×10^{10} particles/mL for the dispersions of 2, 10, 20, and 40 nm Au colloids, respectively. Their pH values are about 7.0. Preparation of Fe_3O_4 colloids was described in the Experimental Section.

of 14 nm (Figure 3c). The yellow free-standing film had a thickness of 60 nm, when prepared from 15 mL of nanostrand solution and 0.15 mL of 1 mM DY solution. The nanocomposite film containing EB (Evans blue) was shown in Figure 3d. In this case, the film was prepared from 5 mL of nanostrand solution. The resultant free-standing film has a thickness of only 20 nm. However, the film was very stable on the centimeter scale and readily peeled off from the substrate. Because of the extremely high molar absorption coefficient ($\epsilon = 78100$ $L \cdot mol^{-1} \cdot cm^{-1}$ at 628 nm),[23] the film appears dark blue.

The films prepared by filtration have pores in the range of several to tens of nanometers. The nanofibrous bundles deposit one by one in a random way, forming a stable network structure. In the case of EB/nanostrand composite films, the nanofibers with an average width of 15 nm gave a uniform film on the centimeter scale. This nanofiber might have a rectangular cross-section, and the short site is no more than 10 nm. Even in such a case, the thickness of this film (20 nm) corresponds to just a few layers of the nanofibers. It should be stressed that the filtration technique can deposit the nanofibers very evenly and uniformly. Furthermore, just a few layers of nanofibers can provide a film that is tough enough to be free-standing on the centimeter scale.

The nanofibrous composite films that peeled off in ethanol were readily transferred, without any damage, onto a glass slide by immersing it under a floating film and slowly lifting (see Supporting Information). The transfer onto a porous alumina membrane was much easier. Figure 4a shows the cross-sectional SEM image of EB/nanostrand film on the alumina membrane. The film was very uniform over a wide area of the substrate. The enlarged image is shown in Figure 4b. The thickness was estimated to be 20 ± 3 nm, after subtracting the thickness of surface platinum layer. From the image, it is clear that the film is made of a few layers of nanofibers. As shown in Figure 4c, the thickness of EB/nanostrand films linearly increased with the volume of filtered dispersion. The short error bars indicate the uniformity of EB/nanostrand films. When a 1.9 cm filtration funnel was used, the lowest thickness was 20 nm, and there was no limitation in the thickness at least up to several micrometers. When the film was thick, the longer filtration time was required. In our experimental conditions, it took 15 min

(23) Roberts, W. G.; Palade, G. E. *J. Cell Sci.* **1995**, *108*, 2369.

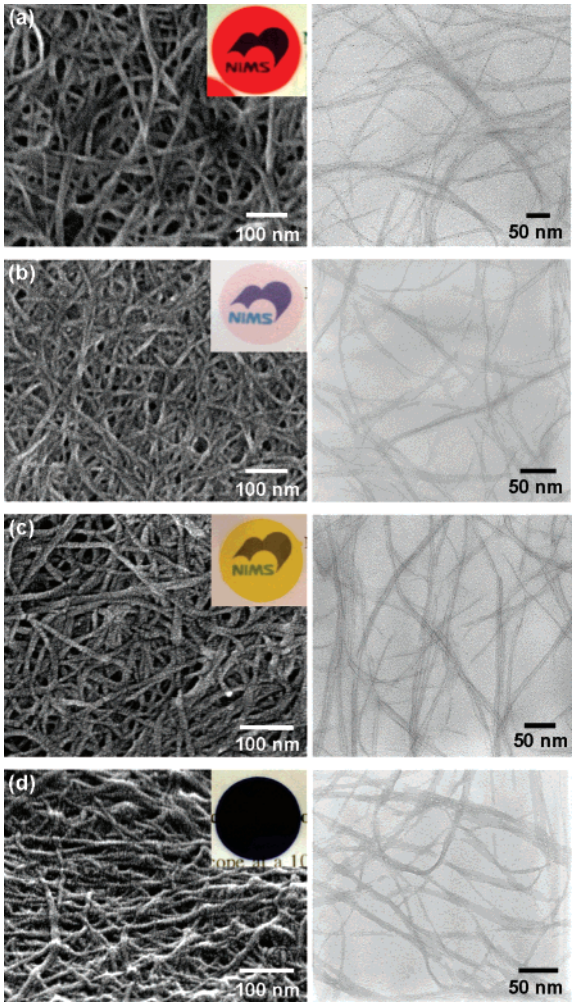

Figure 3. SEM and TEM images of nanofibrous composites containing CR (a), DATS (b), DY (c), and EB (d). The insets in SEM images show the corresponding photographs of the films after peeling off from the substrate in ethanol. These films correspond to CR-3, DATS, DY-2, and EB-1 in Table 1.

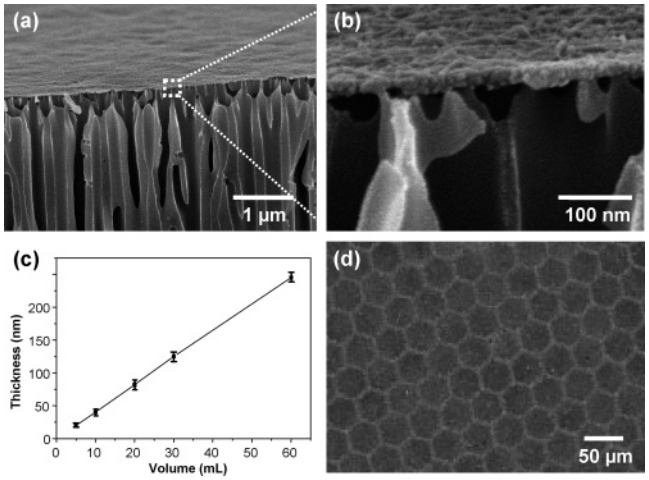

Figure 4. Cross-sectional SEM images of EB/nanostrand film at low (a) and high (b) magnification, the thickness increase against filtration volume (c), and SEM image of 40 nm thick film transferred on 600-mesh copper grid (d). All images were obtained after coating 2 nm thick platinum.

for the preparation of an EB/nanostrand film of 245 nm. Figure 4d shows an SEM image of a 40 nm thick film transferred on a 600-mesh copper grid. The hexagonal pores of 37 micrometers were fully covered by the film without forming cracks and deflection.

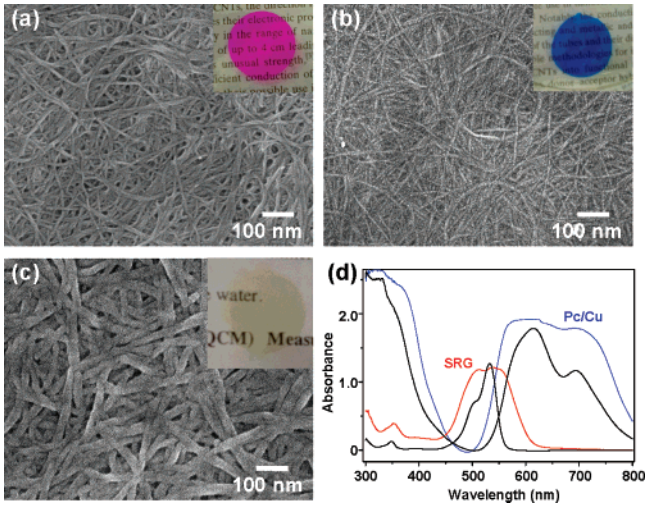

Figure 5. SEM images of nanofibrous composites containing SRG (a), Pc/Cu (b), ANTS (c), and UV−vis absorption spectra of SRG and Pc/Cu (d). The insets in (a−c) are the photographs of the corresponding free-standing films. The spectra of the films containing SRG and Pc/Cu are red and blue, respectively. The black lines are the corresponding spectra of the aqueous solutions (0.02 mM). The preparation conditions are denoted in Table 1.

Sulforhodamine G (SRG) has one negative charge at neutral pH. It was also possible to incorporate such dye into nanofibrous free-standing films. As shown in Figure 5a, the film on a PC membrane was composed of nanofibers with a width of 17 nm. The apparently flexible fibers formed pores of a few tens of nanometers. The pink free-standing film that peeled off from the substrate was very transparent. Pc/Cu formed little narrow nanofibers of 10 nm. They gave a blue, transparent, free-standing film. In contrast to Pc/Cu, ANTS gave the widest nanofibers of 32 nm. The film showed slight green color. It should be again stressed that a 42 nm thick free-standing film was obtained from the nanofibers of 32 nm in width. The tapelike nanofibers can uniformly deposit on a PC membrane filter by filtration.

These films were transferred onto a quartz slide and subjected to spectroscopic measurements. Figure 5d shows the UV−vis absorption spectra of the free-standing films containing SRG (red line) and Pc/Cu (blue line). The former film had the absorbance near 520 nm, much wider than that of the aqueous solution of SRG (black line). Similar broadening was observed for the film containing Pc/Cu. These data suggest that SRG and Pc/Cu aggregate in each composite film. Furthermore, the dye molecules should have some different arrangements to give blue and red shifts. ANTS/nanostrand film also showed significant broadening in the absorption spectra. SRG, Pc/Cu, and ANTS are fluorescent dyes. However, the fluorescence of these free-standing films was completely depressed due to the concentration quenching.

All the dyes shown in Figure 2 seem to aggregate in the nanofibrous composites. In such cases, the electrostatic interaction with the nanostrands must be very strong. The dye molecules also contribute to the stabilization of the free-standing films, since the films consisting only of cadmium hydroxide nanostrands are fragile and they are not free-standing on the centimeter scale. As listed in Table 1, the filtration method

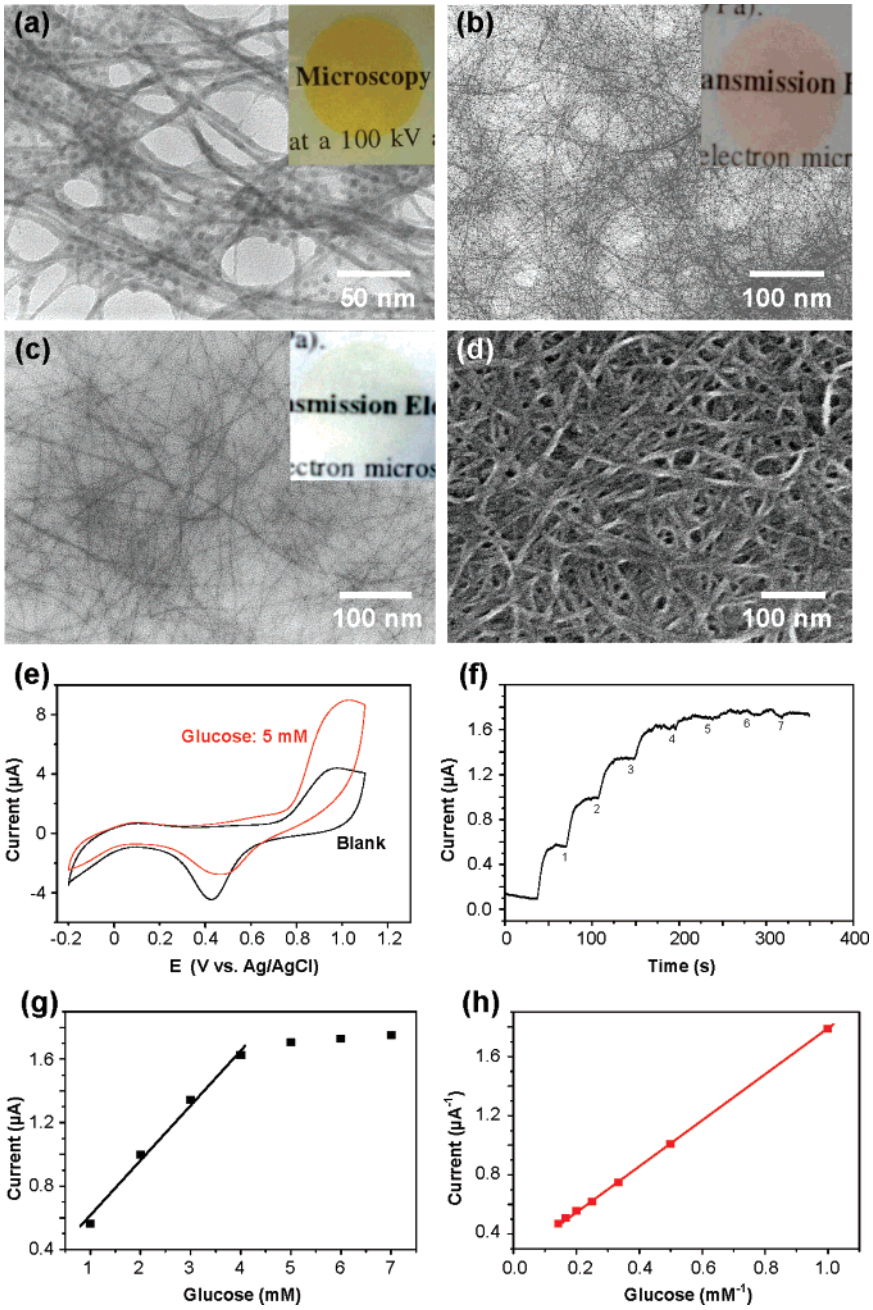

Figure 6. TEM images of nanofibrous composites containing ferritin (a), Cyt.c (b), GOx (c). SEM image of the GOx composite (d) and electrochemical properties of free-standing GOx/nanostrand films (e−h). The insets in (a−c) are photographs of the free-standing films after being transferred onto a quartz plate. The cyclic voltammetric curves in part e were obtained for the film transferred onto a gold electrode. The red and black curves are obtained in phosphate buffer solutions with and without 5 mM glucose. The amperometric response (f) was measured at 0.9 V (vs Ag/AgCl) for successive addition of seven aliquots of glucose solution under stirring at 300 rpm. The current increase against glucose concentration and the Lineweaver−Burk plot are shown in parts g and h.

provides various free-standing films in the range of a few tens to several hundreds of nanometers. Simplicity and generality of this method should be advantages that are hard to see in other methods, such as layer-by-layer adsorption and Langmuir−Blodgett techniques.

Free-Standing Films of Protein/Nanostrand Composites. Subsequently, we examined the incorporation of water-soluble proteins into nanofibrous free-standing films. The first example is the composite of ferritin and cadmium hydroxide nanostrands. Ferritin is a large protein with a diameter of about 12 nm, and it has a hydrated iron oxide core of 6 nm in its inside. The isoelectric point is pH 4.5−4.8, so that this protein is negatively charged in neutral conditions.[24] The aqueous solution (1 mg/mL) was mixed with the nanostrand solution (10 mL), and then slowly stirred for 30 min. TEM observation of this mixture revealed that the nanostrand and ferritin assembled each other to give a network structure (Figure 6a). The yellow free-standing film was highly transparent, which indicated the protein was uniformly dispersed in the film.

Figure 6b,c shows TEM images of nanofibrous composites of cytochrome c (Cyt.c) and glucose oxidase (GOx). The former protein has an isoelectric point at pH 10.6, so that the protein

(24) (a) Velev, O. D. *Adv. Biophys.* **1997**, *34*, 139. (b) Cohen, S.; Vernier, R. L.; Michael, A. F. *Am. J. Pathol.* **1983**, *110*, 170.

solution was first adjusted to pH 11.0. As a result, we could successfully incorporate Cyt.c into the free-standing film without disrupting cadmium hydroxide nanostrands. The protein was invisible in the TEM image. However, UV−vis absorption spectra of the slightly red film gave a strong peak at 407 nm, which was consistent with the absorption peak of native Cyt.c.[25] Incorporation of GOx was also confirmed by the absorption peaks at 382 and 452 nm.[26] They were exactly same as the peaks observed for the aqueous solution of GOx, indicating the protein was not denatured in the free-standing film. The width of the nanofibrous composite of GOx and cadmium hydroxide nanostrand was about 10 nm after subtracting the thickness of platinum layer (Figure 6d). The bundlelike structures were not observed by TEM. Therefore, we concluded that GOx adsorbed on the surface of the nanostrand. Judging from the dimension of GOx ($7.0 \times 5.5 \times 8.0$ nm^3)[27] and the width of the nanostrand (1.9 nm), GOx seems to adsorb lineally along the nanostrand.

The enzymatic activity of GOx was examined by an electrochemical method. A free-standing film containing GOx was prepared at the condition listed in Table 1. The film was transferred on the tip of a gold rod electrode of 2 mm in diameter, and dried for 30 min in argon atmosphere. Cyclic voltammetric measurements were conducted in phosphate buffer by using a platinum counter electrode and an Ag/AgCl reference electrode. Figure 6e shows the results obtained with and without 5 mM glucose. The clear increase of current between 0.8 and 1.1 V indicates that GOx oxidized glucose and hydrogen peroxide generated near the working electrode.[28] The hydrogen peroxide decomposed to oxygen, producing two electrons. It is apparent that GOx immobilized in the nanofibrous free-standing films keeps enzymatic activity. The amperometric response obtained by increasing the concentration of glucose from 0 to 7 mM is shown in Figure 6f. The response was quick and completed within 15 s. The change in current in each step occurred by the increase of glucose concentration of 1 mM. We plotted these changes against the glucose concentration. Furthermore, the relationship between current and glucose concentration was converted to a Lineweaver−Burk plot. These are shown in Figure 6g,h. The response current increased with the concentration of glucose up to 5 mM. The linear range was shown by a black line in Figure 6g. From the slope of this line and the area of the gold electrode (0.0314 cm^2), we calculated the sensitivity to be 9.86 μA/cm^2·mM. This sensitivity is considerably high as compared with the values reported for the GOx immobilized on titania films,[28] carbon nanotubes,[29] and other substrates.[30] The apparent Michaelis−Menten constant (K_m), which is a measure of the enzymatic affinity, was calculated to be 6.11 mM according to the following equation

$$1/I = (K_m/I_{max})\,(1/S) + 1/I_{max} \qquad (1)$$

where I is the current, I_{max} is the maximum current, and S is the glucose concentration. The calculated value was comparable

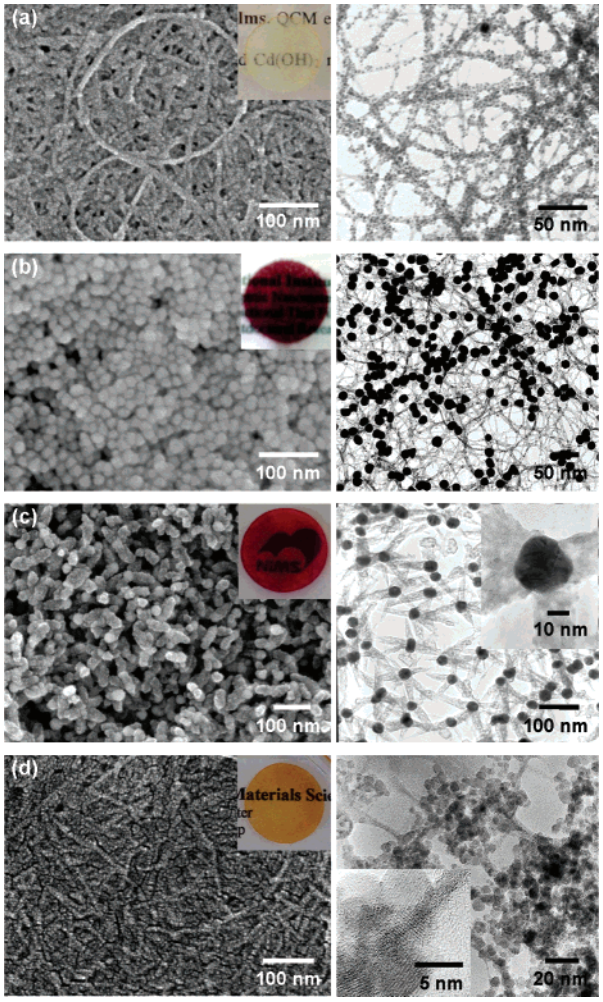

Figure 7. SEM and TEM images of nanocomposites containing Au (a−c) and Fe_3O_4 (d) nanoparticles. The insets in SEM images are the photographs of their free-standing films. The preparation conditions of these samples are corresponding to Au-2, Au-5, Au-7, and Fe_3O_4 in Table 1.

to those reported for native GOx (6.8 mM),[31] GOx immobilized on gold nanoparticles (4.3 mM),[32] and GOx immobilized on a porous titania electrode (6.1 mM),[33] indicating that the high affinity of GOx was kept in the GOx/nanostrand composite films, too. This is probably because the nanostrands provide a proper hydrophilic environment, which prevents GOx from denaturing and ensures a high penetration rate for the water containing glucose.

Free-Standing Films Containing Nanoparticles. The further investigation was conducted for metal and inorganic nanoparticles. The free-standing films obtained by using Au nanoparticles were very uniform. When the size was 2 nm, the nanoparticles adsorbed along the nanostrands, as confirmed by SEM and TEM observations (Figure 7a). The film has nanofibrous morphology with pores of a few to tens of nanometers.

(25) Oellerich, S.; Wackerbarth, H.; Hildebrandt, P. *J. Phys. Chem. B* **2002**, *106*, 6566.
(26) Shin, K.-S.; Youn, H.-D.; Han, Y.-H.; Kang, S.-O.; Hah, Y. C. *Eur. J. Biochem.* **1993**, *215*, 747.
(27) (a) Hecht, H. J.; Schomburg, D.; Kalisz, H.; Schmid, R. D. *Biosens. Bioelectron.* **1993**, *8*, 197. (b) Gooding, J. J.; Situmorang, M.; Erokhin, P.; Hibbert, D. B. *Anal. Commun.* **1999**, *36*, 225.
(28) (a) Yu, J.; Liu, S.; Ju, H. *Biosens. Bioelectron.* **2003**, *19*, 401. (b) Lin, Y.; Lu, F.; Tu, Y.; Ren, Z. *Nano Lett.* **2004**, *4*, 191.
(29) Callegari, A.; Cosnier, S.; Marcaccio, M.; Paolucci, D, Paolucci, F.; Georgakilas, V.; Tagmatarchis, N.; Vázquez, E.; Prato, M. *J. Mater. Chem.* **2004**, *14*, 807.
(30) (a) Lumley-Woodyear, T.; Rocca, P.; Lindsay, J.; Dror, Y.; Freeman, A.; Heller, A. *Anal. Chem.* **1995**, *67*, 1332. (b) Wang, B.; Li, B.; Deng, Q.; Dong, S. *Anal. Chem.* **1998**, *70*, 3170.
(31) Kamln, R. A.; Wilson, G. S. *Anal. Chem.* **1980**, *52*, 1198.
(32) Zhang, S.; Wang, N.; Yu, H.; Niu, Y.; Sun, C. *Bioelectrochemistry* **2005**, *67*, 15.
(33) Li, Q.; Luo, G.; Feng, J.; Zhou, Q.; Zhang, L.; Zhu, Y. *Electroanalysis* **2001**, *13*, 413.

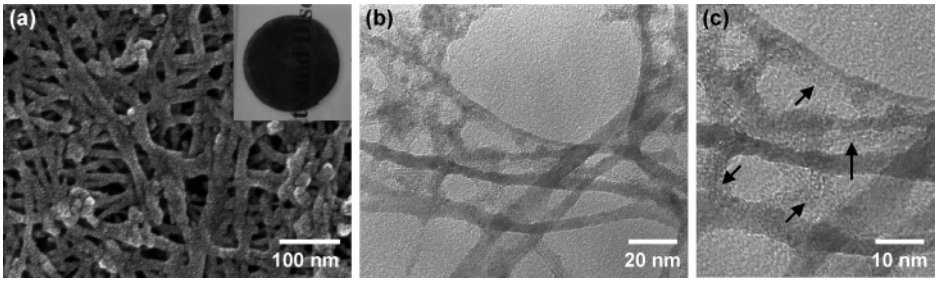

Figure 8. SEM (a) and TEM (b, c) images of nanofibrous composites containing CNT. The inset in part a is the free-standing film removed from the substrate. These images correspond to CNT-1 in Table 2.

The density of the immobilized nanoparticles could be adjusted by choosing the volume of the colloidal dispersion. In the cases of 10 nm (see Supporting Information), 20 nm (Figure 7b), and 40 nm Au nanoparticles (Figure 7c), several nanostrands adsorbed around a nanoparticle, forming a network structure. The SEM images appear just like granular deposits. However, actually, the nanoparticles are isolated from each other, acting as connectors for the nanostrands. The bigger the nanoparticles were, the more the nanostrands connected on them. When the nanoparticles were 40 nm in diameter, a few nanostrands got started forming a bundle, as confirmed by TEM observation (Figure 7c). The high-resolution TEM image clearly showed the lattice structures of gold and cadmium hydroxide nanostrands. The photographs of these free-standing films were transparent and showed colors very close to those in solutions. This strongly indicates that individual Au nanoparticles are isolated from each other in the films.

It was also possible to introduce magnetic nanoparticles into free-standing films. We prepared negatively charged Fe_3O_4 particles with an average diameter of 5 nm. Figure 7d shows the SEM image of the composite film on a PC membrane filter and the corresponding TEM image obtained from the aqueous dispersion. Similarly to the case of 2 nm Au nanoparticles, 5 nm Fe_3O_4 nanoparticles absorbed along the nanostrands and gave a film with nanofibrous morphology. The inset in the SEM image shows the photograph of a 45 nm thick free-standing film. The transparent yellow film could be moved under an external magnetic field, as seen in the movie included as Supporting Information.

Free-Standing Films Containing Fullerene and Carbon Nanotubes. Finally, the incorporation of negatively charged water-soluble fullerene (C_{60}) and single-walled carbon nanotubes (CNTs) were examined. The preparation of these materials is described in detail in the Experimental Section, and the preparation conditions of the free-standing films are described in Table 2. The former C_{60}/nanostrand composites gave a nanofibrous film very close to the film made with 2 nm Au nanoparticles (see Supporting Information). The film was transparent and could be transferred onto a glass substrate. The TEM image indicated that the C_{60} was prone to form aggregates and adsorbed along the nanostrands. The film thickness could be controlled by choosing the volume of the aqueous dispersions of the composites, as shown in Table 2.

Negatively charged single-walled carbon nanotubes were prepared by oxidation with nitric acid. Therefore, the surfaces are supposed to have many carboxyl groups. The composite films with cadmium hydroxide nanostrands are shown in Figure 8. The 60 nm thick dark brown film was transparent and free-standing although the uniformity was not so high. The TEM image revealed that CNT formed the bundles of 5 nm or so, as shown by arrows in Figure 8c. The nanostrands also formed the bundles probably due to the electrostatic interaction with negatively charged CNT.

Table 2. Preparation of Ultrathin Free-Standing Films Containing C_{60} and CNT

sample	concentration	volume (mL)	nanostrand solution (mL)	nanofiber width (nm)	funnel diameter (cm)	thickness (nm)	corresponding images
C_{60} Solution							
C_{60}-1	0.3 mM	0.4	20	7	1.9	85	Figure S4a−c
C_{60}-2	0.3 mM	0.3	15	7	1.9	65	none
C_{60}-3	0.3 mM	0.15	10	7	1.9	42	none
SWCNT Solution							
CNT-1	0.2 mg/mL	1.5	13.3	8	1.9	60	Figure 8a−c
CNT-2	0.2 mg/mL	2.5	20	8	1.9	110	none

Conclusions

We have demonstrated a general method for the preparation of ultrathin nanofibrous free-standing films. We stress that centimeter scale films were obtained despite the thickness of a few tens of nanometers. The films prepared by filtration were very uniform. Especially, an EB/nanostrand composite gave a 20 nm thick film composed of a few layers of the nanofibers. The size was 1000000 times larger than the thickness. Such films can be formed because of the long and narrow structure of the nanofibers. Our results verified, for the first time, the toughness of nanometer-thick nanofibrous composite films, although the mechanical strength has not been examined. The concentration of dyes in the nanocomposite films was extremely high. This is due to the high positive charge density at the surfaces of cadmium hydroxide nanostrands. It should be impossible to achieve such incorporation by using polymer thin films and other matrices like carbon nanotubes. The nanostrands could incorporate plenty of globular particles. As seen in the cases of Au nanoparticles, it gave an interesting network structure, in which the nanoparticles exist densely and isolated from others.

The filtration technique is versatile. In this article, we have applied it to a wide range of charged materials. The technique is also useful for the layer-by-layer deposition of nanofibrous composite materials. In other words, various nanofibrous multilayers are readily prepared just by choosing the order of the filtered solutions. The technique is very simple and speedy, as compared with spin coating, LB techniques, alternate adsorption of polyelectrolytes, etc. A disadvantage is the toxicity of the cadmium atom. However, we have reported that copper

hydroxide gives a nanostrand very close to that of cadmium hydroxide.[21] More recently, we found that zinc hydroxide forms the nanostrand, too. These new inorganic nanostrands will be more suitable for biorelated applications.

In general, the films formed from nanofibrous composites have many mesoscopic pores, due to the rigidity of the nanocomposite fibers. It will be hard to form such a porous structure by using flexible polymers.[8,16] We have demonstrated that a GOx-immobilized free-standing film became a highly sensitive glucose sensor. The high porosity was favorable for glucose to access the immobilized enzymes. The network structure induced by Au nanoparticles should provide much higher permeability for molecules. Such free-standing films seem to be useful for designing various catalysts and gas sensors.[34]

Furthermore, we have succeeded in the preparation of free-standing films without using the sacrificial layer. This is very important for the scale-up of a manufacturing process. The filtration-based technique has great potential to be a continual manufacturing process just like the production of paper. The large scale manufacture of ultrathin nanofibrous free-standing films with mesoscopic pores and the permeation of biomacromolecules are now being investigated in our group.

Experimental Section

Materials. $CdCl_2 \cdot 2.5H_2O$, $FeCl_2 \cdot 4H_2O$, $FeCl_3 \cdot 6H_2O$, 2-aminoethanol, ammonia solution (28%), tetrabutylammonium hydroxide, *p*-sulfobenzoic acid potassium salt, congo red, direct yellow 50, Evans blue, dihydroxy-1,1′-azonaphthalene-3,3′,6,6′-tetrasulfonic acid tetrasodium salt, and 8-aminonaphthalene-1,3,6-trisulfonic acid disodium salt were purchased from Kanto Chemical. Sulforhodamine G, copper phthalocyanine tetrasulfonic acid tetrasodium salt, glucose oxidase, cytochrome c, and horse spleen ferritin were purchased from Sigma-Aldrich. Au colloids were purchased from British Biocell International. Fullerene (C_{60}, 99.5%) was obtained from Materials and Electrochemical Research Corp. Single-walled carbon nanotubes produced by a high-pressure CO conversion method were purchased from Carbon Nanotechnologies. Deionized water (18.2 MΩ) was produced by a Millipore Direct-Q System, and used throughout the experiments. Polycarbonate (PC) membrane filters (Nuclepore, Whatman) of 2.5, 4.7, and 9.0 cm in diameter were used for the preparation of free-standing films.

Preparation of Fe_3O_4 Nanoparticles. Fe_3O_4 nanoparticles were prepared by modifying the reported method.[35] $FeCl_3 \cdot 6H_2O$ (1.18 g) was dissolved in 40 mL of water and heated up to 60 °C, and then $FeCl_2 \cdot 4H_2O$ (0.43 g) was added under stirring. After quickly adding 1 mL of 28% ammonia solution, the mixture was heated at 80 °C for 1 h. The nanoparticles were captured by magnets and washed with 20 mL of deionized water 5 times, and then dispersed in 80 mL of water by ultrasonification. Into one-half of the above solution, *p*-sulfobenzoic acid potassium salt (0.61 g) was dissolved. The carboxyl group of this compound binds to the Fe_3O_4 nanoparticle. The resultant nanoparticles were isolated by magnet, washed with adequate water, dispersed in 250 mL of water at pH 6.4, and used for the preparation of nanofibrous free-standing films.

Preparation of Water-Soluble Fullerene. The water-soluble fullerene was synthesized by the method reported by Wilson et al.[36] First, C_{60} (9 mg) was dispersed in 10 mL of toluene and sonicated until it was completely dissolved. The purple solution was then vigorously stirred after adding 10 mL of aqueous sodium hydroxide (containing 6.6 g NaOH) and 1 mL of 40% tetrabutylammonium hydroxide. Discoloration of the toluene layer occurred within a few min. After 30 min, the mixed solution was allowed to stand to form a black gelled part at the water/toluene interface. The nearly colorless toluene layer was then carefully removed by decantation, and the remaining aqueous layer was vigorously stirred for 2 days under an oxygen sparge at room temperature. Then, 60 mL of methanol was added to the reaction flask, resulting in precipitation of the C_{60} material and excess sodium hydroxide. The mixture of brown and white precipitates was collected by centrifuge and washed with 100 mL of methanol. The solid was redissolved in 20 mL of deionized water, and the resulting solution was precipitated again by the addition of methanol. This procedure was repeated 7 times. After the final centrifuge separation, the precipitation was dissolved in 15 mL of water. The resultant solution (pH 8.5) contains 0.6 mg of Na^+-fullerenol.

Preparation of Water-Soluble CNT. The water-soluble CNT was prepared by partial oxidation using nitric acid.[37] A certain amount of single-walled carbon nanotubes was heated in 6 M nitric acid at 80 °C for 24 h. The solution was subsequently washed with adequate deionized water, and the precipitates were collected by centrifuge. The washing and centrifugation were repeated several times until the solution reached pH 6.5. The resultant materials were dispersed in water by sonication to give a concentration of 0.2 mg/mL, and used for the preparation of nanofibrous free-standing films.

Characterization. The films were characterized by using a scanning electron microscope (SEM, Hitachi S-4800), a transmission electron microscope (TEM, JEOL 1010), and a high-resolution transmission electron microscopy (HR-TEM, JEM 2100F) equipped with an energy-dispersive X-ray analysis system. The specimens for TEM and HR-TEM observation were prepared by floating a carbon-coated TEM grid on each sample solution for a few seconds, wiping the solution from the edge of the grid, and then drying in vacuum. SEM observation was conducted after coating 2 nm thick platinum layer by using a Hitachi e-1030 ion sputter at the pressure of 10 Pa and the current density of 10 mA. UV−vis absorption spectra were obtained by using a SHIMAZU UV-3150 spectrophotometer. The photoluminescence spectra were obtained by a JASCO FP-6500 spectrofluorometer.

Electrochemical Experiments. The electrochemical characterization of GOx/ nanostrand composite films was carried out by using a potentiostat/galvanostat system (Autolab, type III). The measurements were conduced in phosphate buffer solution (50 mM KH_2PO_4 solution, pH was adjusted to 7.4 with H_3PO_4) at room temperature. The scan speed of cyclic voltammetric measurements was 50 mV/s.

Supporting Information Available: Additional details on the transfer of dye-incorporated films onto glass slides, incorporation of Au nanoparticles, free-standing film containing ferromagnetic nanoparticles, and free-standing films containing water-soluble fullerene (PDF); movie showing the manipulation of the freestanding film containing ferromagnetic nanoparticles with an external magnetic field (MPEG). This material is available free of charge via the Internet at http://pubs.acs.org.

JA0718974

(34) (a) Daniel, M.-C.; Astruc, D. *Chem. Rev.* **2004**, *104*, 293. (b) Xu, C.; Su, J.; Xu, X.; Liu, P.; Zhao, H.; Tian, F.; Ding, Y. *J. Am. Chem. Soc.* **2007**, *129*, 42. (c) Star, A.; Joshi, V.; Skarupo, S.; Thomas, D.; Gabriel, J. C. P. *J. Phys. Chem. B* **2006**, *110*, 21014. (d) Joseph, Y.; Guse, B.; Yasuda, A.; Vossmeyer, T. *Sens. Actuators, B* **2004**, *98*, 188. (e) Dobrokhotov, V. V.; McIlroy, D. N.; Norton, M. G.; Berven, C. A. *Nanotechnology* **2006**, *17*, 4135.

(35) Jin, J.; Iyoda, T.; Cao, C.; Song, Y.; Jiang, L.; Li, T. J.; Zhu, D. B. *Angew. Chem., Int. Ed.* **2001**, *40*, 2135.

(36) Husebo, L. O.; Sitharaman, B.; Furukawa, K.; Kato, T.; Wilson, L. J. *J. Am. Chem. Soc.* **2004**, *126*, 12055.

(37) (a) Kordás, K.; Mustonen, T.; Tóth, G.; Jantunen, H.; Lajunen, M.; Soldano, C.; Talapatra, S.; Kar, S.; Vajtai, R.; Ajayan, P. M. *Small* **2006**, *2*, 1021. (b) Gomathi, A.; Vivekchand, S. R. C.; Govindaraj, A.; Rao, C. N. R. *Adv. Mater.* **2005**, *17*, 2757. (c) Yu, X.; Munge, B.; Patel, V.; Jensen, G.; Bhirde, A.; Gong, J. D.; Kim, S. N.; Gillespie, J.; Gutkind, J. S.; Papadimitrakopoulos, F.; Rusling, J. F. *J. Am. Chem. Soc.* **2006**, *128*, 11199.